Contribution from the Department of Chemistry,
The University of Alberta, Edmonton, Alberta, Canada T6G 2G2

Binuclear Rhodium Complexes: Their Chemistry with Sulfur Dioxide and the Structure of $[Rh_2Cl_2(\mu\text{-}SO_2)((C_6H_5)_2PCH_2P(C_6H_5)_2)_2]$

MARTIN COWIE* and STEPHEN K. DWIGHT

Received August 13, 1979

The "A-frame" complex $[Rh_2(CO)_2(\mu\text{-}Cl)(DPM)_2][B(C_6H_5)_4]$ (DPM = $(C_6H_5)_2PCH_2P(C_6H_5)_2$) undergoes a facile and reversible reaction with SO_2 to yield $[Rh_2(CO)_2(\mu\text{-}Cl)(\mu\text{-}SO_2)(DPM)_2][B(C_6H_5)_4]$. Spectroscopic studies have shown that SO_2 attack occurs directly at the bridging site of the "A-frame" complex. Treatment of a solution of the SO_2 adduct with excess SO_2 in the presence of chloride ion yields a second SO_2 complex, $[Rh_2Cl_2(\mu\text{-}SO_2)(DPM)_2]$, the structure of which is reported. In the absence of chloride ion, formation of the second SO_2 complex occurs in the presence of small amounts of $[RhCl_2(CO)_2]^-$ with the latter functioning as a chloride-transfer agent. Treatment of the second, SO_2-bridged species with CO yields the complex $[Rh_2(CO)_2(\mu\text{-}CO)(\mu\text{-}Cl)(DPM)_2][Cl]$ which can then be readily converted in solution to the dicarbonyl species *cis*-$[Rh_2Cl_2(CO)_2(DPM)_2]$. The reaction of *trans*-$[Rh_2Cl_2(CO)_2(DPM)_2]$ with SO_2 has also been investigated and has been shown to occur by terminal SO_2 attack, forcing the terminal carbonyl and chloro ligands on one Rh atom into the bridging positions. In solution this species then loses Cl^- and rearranges to the complex $[Rh_2(CO)_2(\mu\text{-}Cl)(\mu\text{-}SO_2)(DPM)_2][Cl]$ which can yield $[Rh_2Cl_2(\mu\text{-}SO_2)(DPM)_2]$ by recoordination of Cl^- and subsequent CO loss. The X-ray structural determination of $[Rh_2Cl_2(\mu\text{-}SO_2)(DPM)_2]$ shows this species to be a distorted "A-frame" complex with a symmetrically bridging SO_2 ligand and terminal chloro ligands. The complex crystallizes in the space group C_{2h}^5-$P2_1/c$ in a cell of dimensions a = 18.228 (1) Å, b = 13.526 (1) Å, c = 19.632 (2) Å, and β = 104.72 (1)° with Z = 4. On the basis of 5207 unique reflections, the structure was refined by full-matrix, least-squares techniques to agreement indices of R = 0.058 and R_w = 0.067. Some relevant metrical parameters are Rh–P(av) = 2.331 (9) Å, Rh–S(av) = 2.169 (2) Å, Rh–Cl(av) = 2.342 (2) Å, and Rh–S–Rh = 79.84 (7)°.

Introduction

The cationic "A-frame" species $[Rh_2(CO)_2(\mu\text{-}Cl)(DPM)_2]^+$ (**1**),[1] diagramed below, has been shown to undergo facile, and

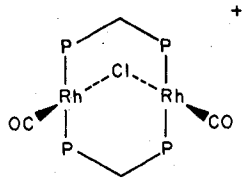

often reversible, reactions with small molecules.[2-4] An X-ray structural determination of **1** as the BF_4^- salt has indicated that both the enclosed bridging site, between the metal centers, and the terminal exposed sites, remote from the bridging site, are open to attack by small molecules.[5] The accessibility of these sites has been confirmed by experiments which have shown that CO attack occurs at the terminal site,[2,4] yielding $[Rh_2(CO)_2(\mu\text{-}CO)(\mu\text{-}Cl)(DPM)_2]^+$ (**2**) (see Scheme I), whereas attack by SO_2[3] (vide infra), PhN_2^+,[1,6] and NO[6] seems to occur directly at the bridging site.

Studies on the coordination of SO_2 in complex **1** indicated that on prolonged treatment of the initially formed SO_2 adduct $[Rh_2(CO)_2(\mu\text{-}Cl)(\mu\text{-}SO_2)(DPM)_2]^+$ (**3**) with SO_2, a disproportionation reaction seemed to occur, yielding the novel "A-frame" species $[Rh_2Cl_2(\mu\text{-}SO_2)(DPM)_2]$ (**4**) and at least one other unidentified species (**5**). The new SO_2-bridged "A-frame" species **4** was subsequently found to exhibit interesting chemistry including CO attack yielding the di- and tricarbonyl species initially assigned as *cis*-$[Rh_2Cl_2(CO)_2(DPM)_2]$ (**6**) and *cis*-$[Rh_2Cl_2(CO)_2(\mu\text{-}CO)(DPM)_2]$ (**7**), respectively.[3,4] A preliminary communication of the above chemistry has appeared.[3] Here we present a detailed report on the structure of complex **4**, on the results and interpretations of further studies on the apparent disproportionation of complex **3**, and on the chemistry of complex **4** with CO, in particular on the nature of the di- and tricarbonyl species **6** and **7**. In addition the chemistry of *trans*-$[Rh_2Cl_2(CO)_2(DPM)_2]$ with SO_2 is outlined.

Scheme I. Reaction of $[Rh_2(CO)_2(\mu\text{-}Cl)(DPM)_2][BPh_4]$ with CO and SO_2

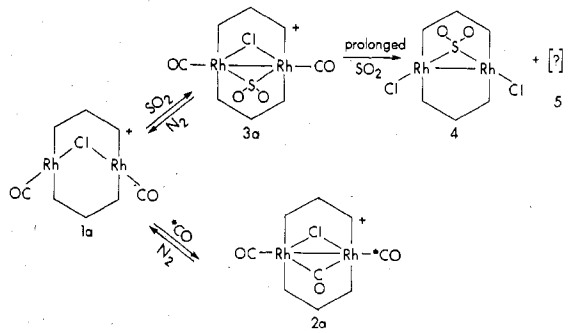

Experimental Section

All solvents were appropriately dried and distilled prior to use under an atmosphere of nitrogen. Reactions were routinely performed under Schlenk conditions with an atmosphere of either nitrogen or the reactant gas. Bis(diphenylphosphino)methane was purchased from Strem Chemicals, and hydrated rhodium chloride was obtained from Research Organic/Inorganic Chemicals. These and all other reagent grade chemicals were used as received. *trans*-$[Rh_2Cl_2(CO)_2(DPM)_2]$[7] and $[RhCl(COD)]_2$[1,8] were prepared by the reported procedures. Infrared spectra were recorded on a Nicolet 7199 F.T. interferometer or on a Perkin-Elmer Model 467 spectrometer using Nujol mulls on KBr plates, and $^{31}P\{^1H\}$ NMR spectra were recorded by using a Digilab pulse Fourier transform-equipped Varian HA-100. Elemental analyses were performed within the department and conductivity measurements were obtained with a Yellow Springs Instrument Model 31 using approximately 1×10^{-3} M solutions in acetone.

Preparation of $Rh_2Cl_2(\mu\text{-}SO_2)(DPM)_2$. Method A. A solution of 0.100 g (0.072 mmol) of $[Rh_2(CO)_2(\mu\text{-}Cl)(DPM)_2][BPh_4]$ in 10 mL of THF[1] was treated with SO_2 for 10 min and then crystallization was induced by addition of diethyl ether saturated with SO_2, yielding red-orange crystals, being analyzed as $[Rh_2(CO)_2(\mu\text{-}Cl)(\mu\text{-}SO_2)(DPM)_2][BPh_4]$, in 90–95% yield. This solid material was redissolved

(1) Abbreviations used: DPM, bis(diphenylphosphino)methane; Ph, phenyl; COD, 1,5-cyclooctadiene; THF, tetrahydrofuran; *t*-Bu, *tert*-butyl; DAM, bis(diphenylarsino)methane.
(2) Cowie, M.; Mague, J. T.; Sanger, A. R. *J. Am. Chem. Soc.* **1978**, *100*, 3628.
(3) Cowie, M.; Dwight, S. K.; Sanger, A. R., *Inorg. Chim. Acta* **1978**, *31*, L407.
(4) Mague, J. T.; Sanger, A. R. *Inorg. Chem.* **1979**, *18*, 2060.
(5) Cowie, M.; Dwight, S. K. *Inorg. Chem.* **1979**, *18*, 2700.
(6) Cowie, M.; Dwight, S. K., to be submitted for publication.
(7) Mague, J. T.; Mitchner, J. P. *Inorg. Chem.* **1969**, *8*, 119.
(8) Chatt, J.; Venuzzi, L. M. *J. Chem. Soc.* **1957**, 4735.

0020-1669/80/1319-0209$01.00/0

Table I. Analytical Data on Complexes

no.	complex	anal., % found C	found H	found Cl	calcd C	calcd H	calcd Cl
2b	$[Rh_2(CO)_2(\mu\text{-}CO)(\mu\text{-}Cl)(DPM)_2][Cl]$	56.39	4.25	6.43	56.36	3.93	6.28
3a	$[Rh_2(CO)_2(\mu\text{-}Cl)(\mu\text{-}SO_2)(DPM)_2][BPh_4]$	62.85	4.44		62.98	4.45	
3b	$[Rh_2(CO)_2(\mu\text{-}Cl)(\mu\text{-}SO_2)(DPM)_2][Cl]$	53.01	4.09		53.58	3.80	
4	$[Rh_2Cl_2(\mu\text{-}SO_2)(DPM)_2]$	54.6	3.80		54.12	4.00	
6	*cis*-$[Rh_2Cl_2(CO)_2(DPM)_2]$	57.37	4.55	6.46	56.70	4.03	6.44

Table II. Spectral and Conductivity Data on the Complexes

no.	complex	IR absn max[a]	assignt	$^{31}P\{^1H\}$/NMR chemical shifts[b]	conductivity,[c] Ω^{-1} cm^2 mol^{-1}
1a	$[Rh_2(CO)_2(\mu\text{-}Cl)(DPM)_2][BPh_4]$[d]	1997 s, 1978 vs	ν_{CO}	16.1 (113.3)	99.0
1b	$[Rh_2(CO)_2(\mu\text{-}Cl)(DPM)_2][Cl]$	1994 s, 1972 vs	ν_{CO}		
2a	$[Rh_2(CO)_2(\mu\text{-}CO)(\mu\text{-}Cl)(DPM)_2][BPh_4]$[d]	1992 s, 1977 vs, 1863 s	ν_{CO}	29.6 (94.2)	94.0
2b	$[Rh_2(CO)_2(\mu\text{-}CO)(\mu\text{-}Cl)(DPM)_2][Cl]$	2004 s, 1960 vs, 1868 s	ν_{CO}	29.8 (94.0)	115.0 (acetone) 49.6 (CH_2Cl_2)
3a	$[Rh_2(CO)_2(\mu\text{-}Cl)(\mu\text{-}SO_2)(DPM)_2][BPh_4]$	2015 s, 1985 s, sh 1229 m, 1070 m	ν_{CO} ν_{SO_2}	24.6 (91.3)	90.0
3b	$[Rh_2(CO)_2(\mu\text{-}Cl)(\mu\text{-}SO_2)(DPM)_2][Cl]$	2010 s, 1985 s, sh 1230 m, 1071 m	ν_{CO} ν_{SO_2}	24.5 (91.6)	65.0
4	$[Rh_2Cl_2(\mu\text{-}SO_2)(DPM)_2]$	1191 m, 1063 m	ν_{SO_2}	19.6 (115.0)	0
6	*cis*-$[Rh_2Cl_2(CO)_2(DPM)_2]$	1971 s	ν_{CO}	19.6 (113.5)	0

[a] Infrared spectra were run as Nujol mulls on KBr plates; vs = very strong; s = strong; m = medium; w = weak; sh = shoulder. [b] $^{31}P\{^1H\}$ NMR chemical shifts are relative to H_3PO_4 (downfield positive), coupling constants ($|^1J_{Rh-P} + {}^xJ_{Rh-P}|$) (in Hz) are given in parentheses. [c] Solvent is acetone unless noted otherwise. [d] References 2 and 4.

in THF and slowly concentrated under a stream of SO_2, yielding the final product as well-formed red-orange crystals, leaving a yellow solution. The yield of this second SO_2 complex was variable, between 0 and 50%, depending on the purity of $[Rh_2(CO)_2(\mu\text{-}Cl)(DPM)_2][BPh_4]$ (vide infra). The elemental analyses for all complexes are shown in Table I and the spectroscopic data and conductivity measurements are given in Table II.

Method B. A suspension of 0.200 g (0.182 mmol) of *trans*-$[Rh_2Cl_2(CO)_2(DPM)_2]$ in 20 mL of CH_2Cl_2 was treated with SO_2 for approximately 2 h. Slow concentration, under a stream of SO_2, yielded the desired crystalline product in 95% yield.

Method C. To a solution of 0.100 g (0.202 mmol) of $[RhCl(COD)]_2$ in 20 mL of CH_2Cl_2 was added 0.156 g (0.405 mmol) of DPM dissolved in 5 mL of benzene. Treatment with SO_2 and concentration of the solution by evaporation under SO_2 yielded the crystalline product $[Rh_2Cl_2(\mu\text{-}SO_2)(DPM)_2]$ in 90% yield.

Preparation of Complexes 1b, 2b, and 6. Treatment of a solution of 0.100 g (0.085 mmol) of complex **4** in 10 mL of either CH_2Cl_2 or acetone with carbon monoxide and concentration under CO yielded quantitatively the product $[Rh_2(CO)_2(\mu\text{-}CO)(\mu\text{-}Cl)(DPM)_2][Cl]$ (**2b**) as an orange microcrystalline solid. Pumping on this solid under vacuum resulted in the total conversion of **2b** to $[Rh_2(CO)_2(\mu\text{-}Cl)(DPM)_2][Cl]$ (**1b**). Bubbling nitrogen through a solution of **2b** followed by slow concentration under nitrogen yielded *cis*-$[Rh_2Cl_2(CO)_2(DPM)_2]$ (**6**) as a yellow crystalline solid.

Spectroscopic Studies on the Stepwise Reactions with SO_2. A solution was prepared by dissolving 0.100 g (0.072 mmol) of **1a** in 3 mL of CD_2Cl_2 in an NMR tube. This was cooled in an 2-propanol/dry ice bath and approximately 0.5 mL of gaseous SO_2 was admitted. The $^{31}P\{^1H\}$ NMR was recorded immediately at 223 K. This procedure was repeated measuring the NMR spectrum after each stepwise addition of SO_2 until nearly all of **1a** had been converted to **3a**. Throughout the runs only signals assignable to **1a** or **3a** were detected.

Infrared spectra were recorded in an analogous manner, by recording the solution infrared spectrum after each stepwise addition of 0.5 mL of SO_2 to a CH_2Cl_2 solution of **1a** (0.500 g (0.361 mmol) in 30 mL). Only bands attributable to complexes **1a**, **3a**, and free SO_2 were detected. The stepwise addition of SO_2 to *trans*-$[Rh_2Cl_2(CO)_2(DPM)_2]$ was similarly monitored by infrared spectroscopy; however, in this case infrared bands at 1740 (m), 1995 (sh), and 2020 (s) cm^{-1} were observed at intermediate times in the experiment. After all of the trans dicarbonyl complex had reacted, only bands attributable to **3b** and free SO_2 were observed (Table II). The NMR and infrared studies on both complexes indicated that several additions of SO_2 were required before any evidence of a reaction was detected.

An NMR spectrum of a sample of **3a** that had disproportionated showed bands assignable to **3a** and **4** as well as bands at $\delta = 8.05$ (s), $\delta = 5.90$ (d, 70 Hz), and $\delta = -13.4$ (d, 120 Hz). The sum of the integrated intensities of the last three peaks was approximately equal to that of **4**.

X-ray Data Collections. Red crystals of $[Rh_2Cl_2(\mu\text{-}SO_2)(DPM)_2]$, suitable for single-crystal X-ray diffraction studies, were supplied by Dr. A. R. Sanger of the Alberta Research Council. Preliminary film data showed that the crystals belong to the monoclinic system with extinctions ($h0l$, l odd; $0k0$, k odd) characteristic of the centrosymmetric space group $P2_1/c$. Accurate cell parameters were obtained by a least-squares analysis of 12 carefully centered reflections chosen from diverse regions of reciprocal space ($50° \leq 2\theta \leq 70°$, Cu $K\alpha_1$ radiation) and obtained by using a narrow X-ray source. See Table III for pertinent crystal data and the details of data collection. The widths at half-height of several strong low-angle reflections (ω scan, open counter) lay in the range 0.10–0.17°.

Data were collected on a Picker four-circle automated diffractometer equipped with a scintillation counter and a pulse-height analyzer, tuned to accept 90% of the Cu Kα peak. Background counts were measured at both ends of the scan range with crystal and counter stationary. The intensities of three standard reflections were measured every 100 reflections for $2\theta \leq 100°$ and every 50 reflections for the remainder of the data collection. All three standards were found to remain constant during the entire data collection within 1.4% of the mean. The intensities of 7690 unique reflections ($3° < 2\theta < 123°$) were measured by using Cu Kα radiation. The data were processed in the usual manner with $\sigma(F_o^2)$ calculated by using a value of 0.03 for p.[9] A total of 5207 reflections had $F_o^2 \geq 3\sigma(F_o^2)$ and were used in subsequent calculations. Absorption corrections were applied to the data with Gaussian integration.[10]

Structure Solution and Refinement. The structure was solved by using a sharpened Patterson synthesis to locate the two independent Rh atoms. Subsequent refinements and difference Fourier syntheses

(9) Doedens, R. J.; Ibers, J. A. *Inorg. Chem.* **1967**, *6*, 204.
(10) Besides local programs and some kindly supplied by J. A. Ibers, the following were used in the solution and refinement of the structure: FORDAP, the fourier summation program by A. Zalkin; DATAP, absorption and extinction program by P. Coppens; SFLS-5, structure factor and least-squares refinement by C. J. Prewitt; ORFFE, for calculating bond lengths, angles, and associated standard deviations by W. Busing and H. A. Levy; ORTEP, plotting program by C. K. Johnson.

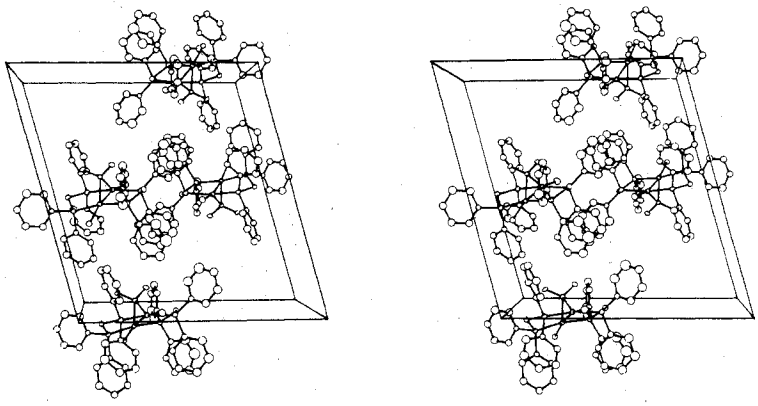

Figure 1. Stereoview of the unit cell of $[Rh_2Cl_2(\mu\text{-}SO_2)(DPM)_2]$. The x axis is horizontal to the right, the z axis runs from bottom to top, and the y axis goes into the page. Vibrational ellipsoids of 20% probability are used on all drawings, unless otherwise noted, with the exception of the methylene hydrogen atoms which are drawn artificially small.

Table III. Summary of Crystal Data and Intensity Collection

compd	$Rh_2Cl_2(\mu\text{-}SO_2)(DPM)_2$
formula	$C_{50}H_{44}Cl_2O_2P_4Rh_2S$
fw	1109.58
a, Å	18.228 (1)
b, Å	13.526 (1)
c, Å	19.632 (2)
β, deg	104.72 (1)
V, Å^3	4681.6
Z	4
dens, g cm^{-3}	1.574 (calcd) 1.59 (2) (exptl)
space group	C_{2h}^5-$P2_1/c$
cryst dimens mm	0.31 × 0.21 × 0.06
cryst vol, mm^3	0.0025
cryst shape	monoclinic prism with {100}, {001}, {110}, and {$\bar{1}$10} faces well developed
radiation	Cu Kα (λ 1.540 56 Å)
temp, °C	20
μ, cm^{-1}	89.55 cm^{-1}
absn cor factors (as applied to F's)	0.479–0.837
receiving aperture	3 mm × 3 mm, 30 cm from the crystal
takeoff angle, deg	2.6
scan speed	2° min^{-1} ($3° \leq 2\theta \leq 100°$); then 1° min^{-1} ($100 < 2\theta \leq 123°$)
scan range	0.75° below Kα_1 to 0.75° above Kα_2
bkgd counting	10 s ($3° \leq 2\theta \leq 76°$); 20 s ($76° < 2\theta \leq 100°$); 40 s ($100° < 2\theta \leq 123°$)
2θ limits, deg	3.0–123.0
final no. of variables	216
unique data used ($F_o^2 \geq 3\sigma(F_o^2)$)	5207
error in observn of unit wt	2.199
R	0.058
R_w	0.067

led to the location of all remaining atoms. Atomic scattering factors were taken from Cromer and Waber's tabulation[11] for all atoms except hydrogen for which the values of Stewart et al.[12] were used. Anomalous dispersion[13] terms for Rh, P, Cl, and S were included in F_c. The carbon atoms of all phenyl groups were refined as rigid groups having D_{6h} symmetry and C–C distances of 1.392 Å. These carbon atoms were given independent isotropic thermal parameters. The hydrogen atoms were included as fixed contributions and not refined. Their idealized positions were calculated from the geometries about the attached carbon atom by using C–H distances of 0.95 Å. These hydrogen atoms were assigned isotropic thermal parameters of 1 Å^2 greater than those of their attached carbon atoms. All other nongroup atoms were refined individually with anisotropic thermal parameters. An isotropic secondary extinction parameter was included and refined. The final model with 216 parameters refined converged to $R = 0.058$ and $R_w = 0.067$.[14] In the final difference Fourier map all of the highest 20 residuals were in the vicinities of the phenyl groups (0.99–0.55 e/Å^3). A typical carbon atom on earlier syntheses had an electron density of about 3.9 e/Å^3.

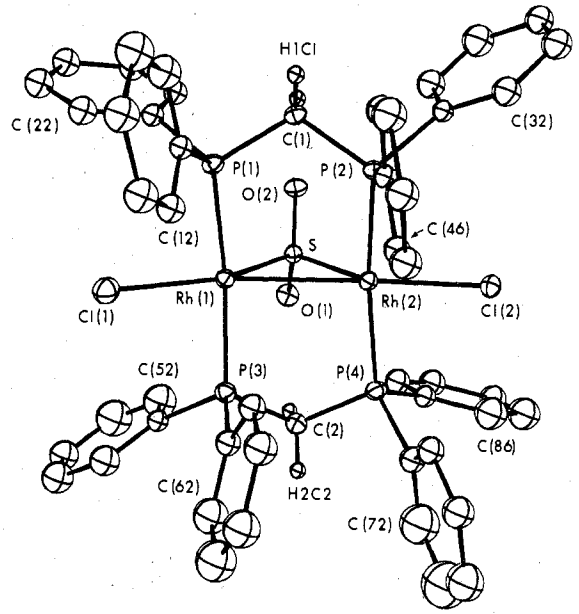

Figure 2. Perspective view of the complex $[Rh_2Cl_2(\mu\text{-}SO_2)(DPM)_2]$ showing the numbering scheme. The numbering on the phenyl carbon atoms starts at the carbon bonded to the phosphorus atom and increases sequentially around the ring.

On the basis of the high thermal parameters of some of these group atoms and the residuals about the phenyl groups, it seems that an anisotropic refinement of the phenyl carbon atoms would have been more suitable. However, this was not attempted due to the very high cost and the feeling that no significant change would result in the parameters of interest.

The final positional and thermal parameters of the nonhydrogen atoms and the group atoms are given in Tables IV and V, respectively. The derived hydrogen positions and their thermal parameters and a listing of the observed and calculated structure amplitudes used in the refinements are available.[15]

Discussion

(a) Description of Structure. The unit cell of $[Rh_2Cl_2(\mu\text{-}SO_2)(DPM)_2]$, shown in Figure 1, contains discrete molecules

(11) Cromer, D. T.; Waber, J. T. "International Tables for X-ray Crystallography"; Kynoch Press: Birmingham, England, 1974; Vol. IV, Table 2.2A.
(12) Stewart, R. F.; Davidson, E. R.; Stewart, W. T. *J. Chem. Phys.* **1965**, *42*, 3175.
(13) Cromer, D. T.; Liberman, D. *J. Chem. Phys.* **1970**, *53*, 1891.

(14) $R = \sum||F_o| - |F_c||/\sum|F_o|$; $R_w = [\sum w(|F_o| - |F_c|)^2/\sum wF_o^2]^{1/2}$.
(15) Supplementary material.

Table IV. Positional and Thermal Parameters for the Nongroup Atoms of $Rh_2Cl_2(\mu\text{-}SO_2)(DPM)_2$

atom	x[a]	y	z	U_{11}[b]	U_{22}	U_{33}	U_{12}	U_{13}	U_{23}
Rh(1)	0.27944 (3)	0.33834 (5)	0.51141 (3)	3.61 (4)	3.37 (4)	3.52 (4)	−0.11 (3)	1.37 (3)	0.04 (3)
Rh(2)	0.21069 (3)	0.16337 (5)	0.45320 (3)	3.41 (4)	3.65 (4)	2.77 (4)	0.05 (3)	0.86 (3)	−0.10 (3)
P(1)	0.16772 (13)	0.42715 (17)	0.50177 (12)	4.10 (12)	3.80 (12)	3.69 (12)	0.19 (10)	1.65 (10)	0.17 (10)
P(2)	0.09370 (12)	0.24418 (17)	0.42655 (12)	3.30 (11)	4.17 (12)	3.20 (12)	−0.05 (10)	1.07 (9)	0.05 (10)
P(3)	0.39565 (13)	0.27382 (17)	0.50565 (13)	3.75 (12)	4.02 (13)	4.77 (14)	−0.06 (10)	1.58 (10)	0.15 (11)
P(4)	0.32324 (13)	0.07714 (18)	0.45789 (13)	4.19 (12)	4.14 (13)	3.90 (14)	0.91 (11)	0.60 (10)	−0.42 (11)
Cl(1)	0.34129 (14)	0.49117 (17)	0.53333 (15)	5.19 (13)	3.99 (12)	8.17 (20)	−0.75 (11)	1.26 (13)	−0.35 (13)
Cl(2)	0.14949 (13)	0.03525 (17)	0.38045 (12)	4.85 (12)	4.83 (13)	4.27 (13)	−1.03 (10)	1.22 (10)	−1.127 (10)
S	0.24409 (12)	0.21097 (16)	0.56221 (11)	4.07 (11)	3.79 (11)	2.75 (11)	−0.11 (9)	1.10 (9)	0.09 (9)
O(1)	0.3057 (4)	0.1574 (4)	0.6091 (3)	5.2 (4)	5.3 (4)	3.2 (3)	0.7 (3)	0.4 (3)	0.9 (3)
O(2)	0.1805 (3)	0.2256 (4)	0.5932 (3)	4.9 (4)	5.6 (4)	3.4 (3)	0.3 (3)	2.4 (3)	0.8 (3)
C(1)	0.0830 (5)	0.3497 (6)	0.4814 (5)	3.5 (4)	4.2 (5)	3.9 (5)	0.4 (4)	1.3 (4)	0.4 (4)
C(2)	0.4077 (5)	0.1385 (6)	0.5106 (5)	4.1 (5)	4.5 (5)	4.4 (6)	0.3 (4)	1.0 (4)	0.2 (4)

[a] Estimated standard deviations in the least significant figure(s) are given in parentheses in this and all subsequent tables. [b] The form of the anisotropic thermal ellipsoid is $\exp[-2\pi^2(a^{*2}h^2U_{11} + b^{*2}k^2U_{22} + c^{*2}l^2U_{33} + 2a^*b^*hkU_{12} + 2a^*c^*hlU_{13} + 2b^*c^*klU_{23})]$.

Table V. Derived Parameters for the Rigid Group Atoms of $Rh_2Cl_2(\mu\text{-}SO_2)(DPM)_2$

atom	x	y	z	B, Å^2	atom	x	y	z	B, Å^2
C(11)	0.1471 (6)	0.5213 (5)	0.4326 (5)	3.4 (2)	C(51)	0.4781 (9)	0.3152 (7)	0.5723 (4)	3.7 (2)
C(12)	0.1927 (5)	0.5318 (5)	0.3860 (4)	4.7 (2)	C(52)	0.531 (1)	0.3813 (7)	0.5592 (7)	7.0 (3)
C(13)	0.1763 (7)	0.6044 (6)	0.3341 (4)	6.1 (3)	C(53)	0.5924 (5)	0.4107 (6)	0.6138 (8)	8.1 (4)
C(14)	0.1142 (6)	0.6666 (5)	0.3288 (5)	6.3 (3)	C(54)	0.6001 (9)	0.3740 (7)	0.6815 (4)	7.3 (3)
C(15)	0.0686 (5)	0.6561 (5)	0.3755 (4)	7.9 (4)	C(55)	0.547 (1)	0.3079 (7)	0.6946 (7)	12.2 (6)
C(16)	0.0850 (7)	0.5835 (6)	0.4274 (4)	6.6 (3)	C(56)	0.4857 (5)	0.2786 (6)	0.6400 (8)	9.7 (5)
C(21)	0.1620 (5)	0.4948 (5)	0.5810 (3)	3.7 (2)	C(61)	0.408 (2)	0.3061 (6)	0.419 (1)	4.3 (2)
C(22)	0.1879 (4)	0.5919 (5)	0.5907 (3)	5.9 (3)	C(62)	0.478 (1)	0.3022 (6)	0.4032 (9)	8.3 (4)
C(23)	0.1933 (4)	0.6390 (4)	0.6548 (4)	6.3 (3)	C(63)	0.483 (2)	0.3235 (6)	0.335 (1)	10.2 (5)
C(24)	0.1726 (5)	0.5892 (5)	0.7091 (3)	6.1 (3)	C(64)	0.419 (2)	0.3488 (6)	0.283 (1)	7.8 (4)
C(25)	0.1467 (4)	0.4921 (5)	0.6994 (3)	5.6 (3)	C(65)	0.348 (1)	0.3527 (6)	0.2994 (9)	6.3 (3)
C(26)	0.1413 (4)	0.4450 (4)	0.6353 (4)	4.5 (2)	C(66)	0.343 (2)	0.3314 (6)	0.367 (1)	4.6 (2)
C(31)	0.0089 (4)	0.1740 (5)	0.429 (1)	3.1 (2)	C(71)	0.349 (1)	0.0554 (7)	0.3747 (5)	4.7 (2)
C(32)	−0.0037 (9)	0.1526 (6)	0.4941 (6)	5.9 (3)	C(72)	0.4136 (9)	0.0005 (7)	0.3759 (8)	11.5 (6)
C(33)	−0.069 (1)	0.1015 (6)	0.4982 (6)	7.6 (4)	C(73)	0.4372 (5)	−0.0123 (6)	0.3144 (9)	14.8 (7)
C(34)	−0.1211 (4)	0.0718 (5)	0.437 (1)	5.8 (3)	C(74)	0.396 (1)	0.0298 (7)	0.2516 (5)	8.7 (4)
C(35)	−0.1086 (9)	0.0932 (6)	0.3715 (6)	6.0 (3)	C(75)	0.3309 (9)	0.0846 (7)	0.2504 (8)	6.0 (3)
C(36)	−0.044 (1)	0.1443 (6)	0.3673 (6)	5.4 (3)	C(76)	0.3073 (5)	0.0974 (6)	0.3119 (9)	4.6 (2)
C(41)	0.0776 (4)	0.2969 (5)	0.3383 (5)	3.2 (2)	C(81)	0.3265 (5)	−0.0469 (5)	0.4969 (5)	4.0 (2)
C(42)	0.0170 (5)	0.3601 (5)	0.3109 (4)	5.0 (2)	C(82)	0.3470 (5)	−0.0588 (5)	0.5698 (4)	5.6 (3)
C(43)	0.0079 (4)	0.4008 (5)	0.2441 (6)	6.0 (3)	C(83)	0.3457 (5)	−0.1523 (7)	0.5990 (3)	6.7 (3)
C(44)	0.0594 (6)	0.3784 (5)	0.2048 (5)	5.2 (2)	C(84)	0.3238 (5)	−0.2340 (5)	0.5553 (5)	6.5 (3)
C(45)	0.1200 (5)	0.3152 (5)	0.2322 (4)	5.2 (2)	C(85)	0.3033 (5)	−0.2220 (5)	0.4825 (4)	9.0 (4)
C(46)	0.1291 (4)	0.2745 (5)	0.2990 (6)	4.1 (2)	C(86)	0.3046 (5)	−0.1285 (7)	0.4533 (3)	8.6 (4)

	rigid group parameters					
group	X_c[a]	Y_c	Z_c	δ[b]	ϵ	η
ring 1	0.1360 (3)	0.5939 (4)	0.3807 (3)	−0.702 (4)	0.864 (6)	4.322 (6)
ring 2	0.1673 (2)	0.5420 (4)	0.6450 (3)	0.339 (5)	1.464 (5)	5.775 (5)
ring 3	−0.0561 (3)	0.1229 (3)	0.4328 (3)	1.049 (4)	1.786 (10)	1.478 (10)
ring 4	0.0685 (3)	0.3376 (3)	0.2715 (3)	2.242 (4)	1.124 (7)	2.452 (7)
ring 5	0.5391 (3)	0.3446 (4)	0.6269 (3)	0.872 (6)	2.146 (8)	5.824 (9)
ring 6	0.4133 (3)	0.3274 (3)	0.3513 (3)	−1.303 (5)	0.617 (19)	4.045 (19)
ring 7	0.3722 (3)	0.0425 (4)	0.3132 (4)	−0.908 (6)	1.453 (9)	2.916 (10)
ring 8	0.3252 (3)	−0.1404 (4)	0.5261 (3)	0.144 (5)	1.853 (5)	1.165 (5)

[a] X_c, Y_c, and Z_c are the fractional coordinates of the centroid of the rigid group. [b] The rigid group orientation angles δ, ϵ, and η (radians) have been defined previously: La Placa, S. J.; Ibers, J. A. *Acta Crystallogr.* **1965**, *18*, 511.

of the complex. Figure 2 presents a perspective view of the compound including the numbering scheme (phenyl hydrogen atoms have the same number as their attached carbon atom). The inner coordination sphere is shown in Figure 3 along with some relevant bond lengths.

The complex $[Rh_2Cl_2(\mu\text{-}SO_2)(DPM)_2]$ displays a distorted "A-frame" geometry, similar to that displayed by the palladium analogue $[Pd_2Cl_2(\mu\text{-}SO_2)(DPM)_2]$[16] (apart from the metal–metal bond in the present species). The "A" configuration is described by the Cl and SO_2 ligands in the equatorial plane, with the apical position occupied by the bridging SO_2 ligand. Both rhodium centers are bridged by two DPM ligands, which are mutually trans and approximately perpendicular to the equatorial plane. The distortion from the idealized "A-frame" structure which would have the terminal Cl ligands trans to the bridging SO_2 ligand results both from close nonbonded contacts between the chloro ligands and the phenyl rings and from the presence of the Rh–Rh bond (see Table VI and Figure 2). Therefore, unlike other "A-frame" complexes which have approximately square-planar coordination at the metals, the present complex exhibits a highly distorted trigonal-bipyramidal metal environment with the average S–Rh–Rh, S–Rh–Cl, and Cl–Rh–Rh angles (50.07 (6), 142.9 (5), and 166.7 (5)°, respectively, see Table VII) deviating significantly from the idealized 120° value.

The Rh–Rh distance of 2.7838 (8) Å is consistent with a normal Rh–Rh single bond, falling within the range previously

(16) Benner, L. S.; Olmstead, M. M.; Hope, H.; Balch, A. L. *J. Organomet. Chem.* **1978**, *153*, C31.

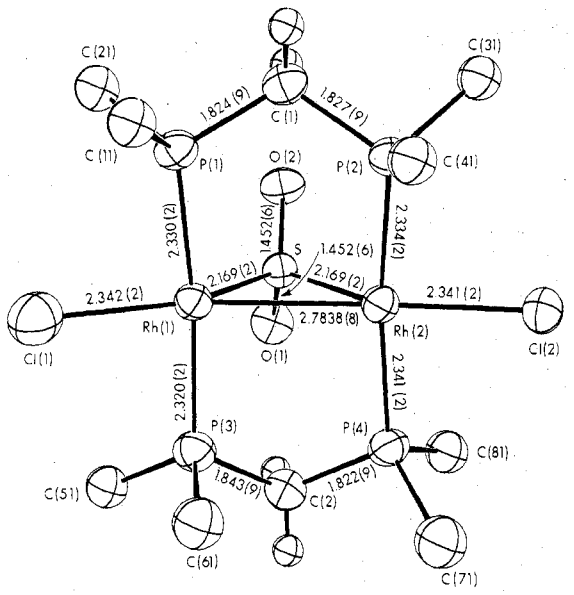

Figure 3. Inner coordination sphere of the complex $[Rh_2Cl_2(\mu\text{-}SO_2)(DPM)_2]$ showing some relevant bond lengths. Only the first carbon atom of each phenyl ring is shown; 50% thermal ellipsoids are used.

Table VI. Selected Distances (Å) in $Rh_2Cl_2(\mu\text{-}SO_2)(DPM)_2$

Bond Distances

Rh(1)-Rh(2)	2.7838 (8)		P(1)-C(1)	1.824 (9)
Rh(1)-S	2.169 (2)		P(2)-C(1)	1.827 (9)
Rh(2)-S	2.169 (2)		P(3)-C(2)	1.843 (9)
Rh(1)-Cl(1)	2.342 (2)		P(4)-C(2)	1.822 (9)
Rh(2)-Cl(2)	2.341 (2)		P(1)-C(11)	1.830 (6)
Rh(1)-P(1)	2.330 (2)		P(1)-C(21)	1.830 (6)
Rh(1)-P(3)	2.320 (2)		P(2)-C(31)	1.824 (5)
Rh(2)-P(2)	2.334 (2)		P(2)-C(41)	1.827 (5)
Rh(2)-P(4)	2.341 (2)		P(3)-C(51)	1.812 (7)
S-O(1)	1.452 (6)		P(3)-C(61)	1.820 (7)
S-O(2)	1.452 (6)		P(4)-C(71)	1.832 (7)
			P(4)-C(81)	1.839 (6)

1.829 (9)

2.331 (9)[a]

1.827 (8)

Nonbonded Distances

P(1)-P(2)	3.018 (3)	O(1)-H1C2	2.52
P(3)-P(4)	3.012 (3)	O(2)-H(45)[b]	2.39
Rh(1)-H(66)	2.70	O(2)-H2C1	2.48
Rh(2)-H(46)	2.73	O(2)-H(26)	2.49
C(52)-H(62)	2.67	H2C1-H(26)	2.15
C(62)-H(52)	2.54	H1C2-H(82)	2.17
O(1)-H(82)	2.43	H(46)-H(76)	2.16
		H(52)-H(62)	2.19

[a] For averaged quantities, the estimated standard deviation is the larger of an individual standard deviation or the standard deviation of a single observation as calculated from the mean. [b] H(45) is associated with the molecule at the general equivalent position $x, {}^1/_2 - y, {}^1/_2 + z$.

Table VII. Selected Angles (deg) in $Rh_2Cl_2(\mu\text{-}SO_2)(DPM)_2$

Bond Angles

Rh(2)-Rh(1)-Cl(1)	166.28 (8)	Rh(1)-P(3)-C(51)	116.6 (3)
Rh(2)-Rh(1)-P(1)	96.43 (6)	Rh(1)-P(3)-C(61)	106.6 (3)
Rh(2)-Rh(1)-P(3)	88.94 (6)	Rh(2)-P(4)-C(71)	117.6 (3)
Rh(2)-Rh(1)-S	50.07 (6)	Rh(2)-P(4)-C(81)	114.0 (3)
Cl(1)-Rh(1)-S	143.33 (9)	C(1)-P(1)-C(11)	103.5 (4)
Cl(1)-Rh(1)-P(1)	85.98 (9)	C(1)-P(1)-C(21)	104.3 (4)
Cl(1)-Rh(1)-P(3)	86.45 (9)	C(1)-P(2)-C(31)	100.1 (4)
P(1)-Rh(1)-P(3)	168.46 (9)	C(1)-P(2)-C(41)	103.8 (3)
P(1)-Rh(1)-S	95.23 (8)	C(2)-P(3)-C(51)	101.7 (4)
P(3)-Rh(1)-S	96.04 (8)	C(2)-P(3)-C(61)	104.3 (4)
Rh(1)-Rh(2)-Cl(2)	167.17 (6)	C(2)-P(4)-C(71)	102.2 (4)
Rh(1)-Rh(2)-P(2)	89.10 (6)	C(2)-P(4)-C(81)	104.2 (4)
Rh(1)-Rh(2)-P(4)	96.25 (6)	C(11)-P(1)-C(21)	103.7 (3)
Rh(1)-Rh(2)-S	50.08 (6)	C(31)-P(2)-C(41)	106.9 (3)
Cl(2)-Rh(2)-S	142.44 (8)	C(51)-P(3)-C(61)	108.9 (4)
Cl(2)-Rh(2)-P(2)	86.75 (7)	C(71)-P(4)-C(81)	103.7 (4)
Cl(2)-Rh(2)-P(4)	86.11 (8)	P(1)-C(11)-C(12)	120.9 (4)
P(2)-Rh(2)-P(4)	169.59 (9)	P(1)-C(11)-C(16)	119.0 (4)
P(2)-Rh(2)-S	95.37 (8)	P(1)-C(21)-C(22)	119.9 (4)
P(4)-Rh(2)-S	94.91 (8)	P(1)-C(21)-C(26)	119.6 (4)
Rh(1)-S-Rh(2)	79.84 (7)	P(2)-C(31)-C(32)	117.9 (4)
O(1)-S-O(2)	111.9 (4)	P(2)-C(31)-C(36)	122.1 (4)
Rh(1)-S-O(1)	114.6 (3)	P(2)-C(41)-C(42)	121.8 (4)
Rh(1)-S-O(2)	116.5 (3)	P(2)-C(41)-C(46)	118.2 (4)
Rh(2)-S-O(1)	117.1 (3)	P(3)-C(51)-C(52)	123.7 (6)
Rh(2)-S-O(2)	113.6 (3)	P(3)-C(51)-C(56)	116.3 (6)
Rh(1)-P(1)-C(1)	113.3 (3)	P(3)-C(61)-C(62)	122.6 (5)
Rh(2)-P(2)-C(1)	117.5 (3)	P(3)-C(61)-C(66)	117.3 (5)
Rh(1)-P(3)-C(2)	117.9 (3)	P(4)-C(71)-C(72)	118.5 (6)
Rh(2)-P(4)-C(2)	113.6 (3)	P(4)-C(71)-C(76)	121.4 (6)
Rh(1)-P(1)-C(11)	115.5 (2)	P(4)-C(81)-C(82)	120.4 (5)
Rh(1)-P(1)-C(21)	115.2 (2)	P(4)-C(81)-C(86)	119.6 (5)
Rh(2)-P(2)-C(31)	118.9 (2)	P(1)-C(1)-P(2)	111.6 (4)
Rh(2)-P(2)-C(41)	108.2 (2)	P(3)-C(2)-P(4)	110.5 (5)

Torsion Angles

P(1)-Rh(1)-Rh(2)-P(2)	6.31 (8)
P(3)-Rh(1)-Rh(2)-P(4)	7.60 (9)
P(1)-Rh(1)-Rh(2)-P(4)	177.36 (9)
P(3)-Rh(1)-Rh(2)-P(2)	163.45 (8)
C(1)-P(1)-P(3)-C(2)	16.2 (5)
C(1)-P(2)-P(4)-C(2)	15.3 (5)
C(11)-P(1)-P(3)-C(61)	18.2 (4)
C(21)-P(1)-P(3)-C(51)	17.9 (4)
C(31)-P(2)-P(4)-C(81)	17.4 (4)
C(41)-P(2)-P(4)-C(71)	17.2 (4)
C(11)-P(1)-P(2)-C(41)	12.2 (3)
C(21)-P(1)-P(2)-C(31)	18.3 (5)
C(51)-P(3)-P(4)-C(81)	20.5 (6)
C(61)-P(3)-P(4)-C(71)	17.1 (4)
C(11)-P(1)-Rh(1)-Cl(1)	60.1 (3)
C(21)-P(1)-Rh(1)-Cl(1)	60.9 (3)
C(31)-P(2)-Rh(2)-Cl(2)	44.8 (3)
C(41)-P(2)-Rh(2)-Cl(2)	77.3 (3)
C(51)-P(3)-Rh(1)-Cl(1)	43.2 (3)
C(61)-P(3)-Rh(1)-Cl(1)	78.5 (3)
C(71)-P(4)-Rh(2)-Cl(2)	60.0 (3)
C(81)-P(4)-Rh(2)-Cl(2)	61.6 (3)

reported for such distances (2.617 (3)–2.8415 (7) Å).[17,18] The present value can be compared to that observed in the related Rh–Rh bonded tricarbonyl species $[Rh_2(CO)_2(\mu\text{-}CO)(\mu\text{-}Cl)(DPM)_2]^+$ (2.8415 (7) Å)[17] and can be contrasted to the distances of 3.1520 (8) and 3.155 (4) Å, respectively, for $[Rh_2(CO)_2(\mu\text{-}Cl)(DPM)_2]^{+}$ [5] and $[Rh_2(CO)_2(\mu\text{-}S)(DPM)_2]$,[19] in which no Rh–Rh bond is present.

The geometry of the bridging SO_2 ligand is consistent with a rhodium–rhodium bonded system. Thus the acute Rh–S–Rh angle of 79.84 (7)° indicates compression along the Rh–Rh axis and is comparable to other such values obtained when SO_2 bridges a metal–metal bond (72.6 (1)–75.6 (2)°)[20–22] but is significantly smaller than the range observed in M–S–M angles (91.2 (2)–118.0 (2)°)[16,23] when SO_2 bridges two metals which are not bonded to each other. The bonding of this SO_2 ligand is symmetric (Rh(1)–S = Rh(2)–S = 2.169 (2) Å) and these Rh–S distances are significantly shorter than the metal–sulfur distances observed in other sulfur dioxide bridged complexes of the second- and third-row platinum metals ($[Pd_2Cl_2(\mu$-

(17) Cowie, M. *Inorg. Chem.* **1979**, *18*, 286 and references therein.
(18) Corey, E. R.; Dahl, L. F.; Beck, W. *J. Am. Chem. Soc.* **1963**, *85*, 1202. Mills, O. S.; Nice, J. P. *J. Organomet. Chem.* **1967**, *10*, 337. Mills, O. S.; Paulus, E. F. *Ibid.* **1967**, *10*, 331. Paulus, E. F. *Acta Crystallogr., Sect. B* **1969**, *25*, 2206. Wei, C. H. *Inorg. Chem.* **1969**, *8*, 2384.
(19) Kubiak, C. P.; Eisenberg, R. *J. Am. Chem. Soc.* **1977**, *99*, 6129.
(20) Meunier-Piret, M.; Piret, P.; Van Meerssche, M. *Bull. Soc. Chim. Belg.* **1967**, *76*, 374. Churchill, M. R.; Kalra, K. L. *Inorg. Chem.* **1973**, *12*, 1650.
(21) Angoletta, M.; Bellon, P. L.; Manassero, M.; Sansoni, M. *J. Organomet. Chem.* **1974**, *81*, C40.
(22) Moody, D. C.; Ryan, R. R. *Inorg. Chem.* **1977**, *16*, 1052.
(23) (a) Churchill, M. R.; DeBoer, B. G.; Kalra, K. L.; Reich-Rohrwig, P.; Wojcicki, A. *J. Chem. Soc., Chem. Commun.* **1972**, 981. (b) Churchill, M. R.; DeBoer, B. G.; Kalra, K. L. *Inorg. Chem.* **1973**, *12*, 1646.

Table VIII. Least-Squares Planes Calculations[a]

plane no.	equation
1	$0.2235X + 0.3314Y - 0.9166Z + 6.7751 = 0.0$
2	$-0.9043X + 0.4149Y - 0.1006Z + 1.3775 = 0.0$
3	$-0.3075X - 0.8651Y - 0.3962Z + 7.2045 = 0.0$

plane no.	dev from planes, Å										
	Rh(1)	Rh(2)	P(1)	P(2)	P(3)	P(4)	C(1)	C(2)	S	O(1)	O(2)
1	−0.0407 (6)	−0.0272 (6)	0.081 (2)	0.352 (2)	0.250 (2)	0.250 (2)	−0.234 (9)[b]	−0.400 (9)[b]			
2	0.0	0.0							0.0		
3									0.0	0.0	0.0

Dihedral Angle between Planes 2 and 3 = 92.35°

[a] *X*, *Y*, *Z* are the orthogonal coordinates (Å) with *X* along the *a* axis, *Y* in the *a*–*b* plane, and *Z* along the *c** axis. [b] Not included in least-squares plane calculations.

$SO_2)(DPM)_2]$, Pd–S = 2.234 (3) and 2.240 (3) Å;[16] $[IrH(CO)_2(PPh_3)]_2SO_2$, Ir–S = 2.313 Å;[21] $[Pt_3(SO_2)_3(PPh_3)_3]$, Pt–S (av) = 2.275 (5) Å;[22] and $[Pd_3(SO_2)_2(t\text{-BuNC})_5]$, Pd–S (av) = 2.261 (9) Å[24]). The S–O distances of 1.452 (6) Å and the O–S–O angle of 111.9 (4)° compare well with other determinations in which SO_2 acts as either a bridging or a terminal ligand[20–25] and can be compared to the analogous parameters in free SO_2 (1.431 (1) Å and 119.0 (5)°, respectively).[26] The differences between coordinated and uncoordinated SO_2 can be attributed to back-donation into SO_2 orbitals which are slightly bonding with respect to the O–O interaction and antibonding with respect to S–O interactions.[25] However, more simply they reflect the change from sp^2 to sp^3 hybridization about the sulfur atom. The Rh–S–O angles are also close to the tetrahedral values.

The Rh–Cl distances of 2.342 (2) and 2.341 (2) Å are not unusual; however, they are somewhat shorter than those typically observed (range 2.355 (2)–2.386 (3) Å)[27,28] for rhodium(I) phosphine complexes.

Within the Rh–DPM framework most parameters are usual. The Rh–P distances (average 2.331 (9) Å) are within the range normally observed when phosphine ligands are mutually trans,[5,16,17,19,28] and the P–C distances (both phenyl and methyl) compare well with other determinations.[5,16,17,19] The methylene carbon atoms of the bridging DPM ligands are folded in a cis configuration toward the sulfur dioxide ligand (see Table VIII and Figure 2). This orientation of the methylene groups allows the phenyl groups to stagger themselves with respect to the terminal chloro ligands in the equatorial plane (see Cl–Rh–P–phenyl torsion angles, Table VII) and also places four of the eight phenyl rings in the open positions around the bridging site. Viewed down the Rh–Rh axis the Rh–P vectors are slightly staggered with respect to one another as can be seen from the P–Rh–Rh–P torsion angles of 6.31 (8)° and 7.60 (9)°. This observed twist in the Rh–DPM framework thrusts rings 4 and 6 further into the enclosed bridging site, effectively blocking this site and resulting in short Rh–H nonbonded contacts (Rh(1)–H(66) = 2.70 Å and Rh(2)–H(46) = 2.73 Å). Although the enclosed site is effectively blocked by these phenyl rings, the exposed terminal sites are conspicuously vacant and open to attack by small molecules.

(b) Transformation of $[Rh_2(CO)_2(\mu\text{-Cl})(\mu\text{-}SO_2)(DPM)_2]^+$ to $[Rh_2Cl_2(\mu\text{-}SO_2)(DPM)_2]$. The reaction of the parent "A-frame" complex, as the BPh_4^- salt, **1a**, with sulfur dioxide yields initially the sulfur dioxide adduct $[Rh_2(CO)_2(\mu\text{-}SO_2)(\mu\text{-Cl})(DPM)_2][BPh_4]$ (**3a**) (see Scheme I). The assignment of this structure is based on (1) the infrared spectrum which is similar to that of the carbonyl adduct **2a**, which has been characterized by an X-ray structural determination,[17] (2) the SO_2 bands in the infrared spectrum, at 1230 and 1070 cm^{-1}, which are in the region observed for other SO_2 ligands bridging metal–metal bonded centers,[21,24] (3) the $^{31}P\{^1H\}$ NMR spectrum which displays only one phosphorus environment, (4) satisfactory elemental analysis, and (5) treatment of a solution of **3a** with nitrogen which leads to loss of SO_2 and isolation of the parent "A-frame" species **1a**.

Prolonged treatment of a solution of **3a** with SO_2 resulted in an apparent disproportionation reaction yielding $[Rh_2Cl_2(\mu\text{-}SO_2)(DPM)_2]$ (**4**) as a red brown microcrystalline material and a yellow solution containing the other disproportionation product(s). Subsequent attempts to repeat the above reaction have shown that it is not a simple disproportionation reaction. When the reaction was repeated by using the pure parent "A-frame", which had been recrystallized several times, it was found that the reaction stopped at the sulfur dioxide adduct **3a**. Whereas when **1a** was purified by only a single crystallization or if the reaction was carried out in situ without purification of **1a**, the transformation of compound **3a** to **4** proceeded to completion in about 4 h. This suggested the involvement of an impurity in the reaction yielding compound **4**.

Since $[Rh(H)Cl(DPM)_2][BPh_4]$ was known to be an impurity in some preparations of **1a**,[29] this species was added to solutions of **3a** to assess its effect on the above reaction. It was found, however, that even when present in equimolar amounts this hydrido complex had no apparent effect on the reaction rate. It should be noted that in the preliminary report[3] of this chemistry, the ^{31}P resonance assigned as the unknown "disproportionation" product (**5**) has now been identified as the above hydride impurity.

Another potential impurity, the $[RhCl_2(CO)_2]^-$ anion, results if exchange of this anion with BPh_4^- is incomplete. To test the possible involvement of the $[RhCl_2(CO)_2]^-$ anion, we treated the complex $[Rh_2(CO)_2(\mu\text{-Cl})(DPM)_2][RhCl_2(CO)_2]$ (**1c**) with SO_2. Regardless of solvent, the transformation of **3** to **4** proceeded to completion in *every* case within 3 h. When traces of **1c** were added to pure **1a**, this reaction again occurred much more readily than with only pure **1a**, suggesting the involvement of the $[RhCl_2(CO)_2]^-$ anion as a chloride transfer agent in the reaction. It has already been shown by Balch and co-workers[30] that the dimer $[RhCl(CO)_2]_2$ abstracts chloride ion from *trans*-$[Rh_2Cl_2(CO)_2(DAM)_2]$[1] to give $[Rh_2(CO)_2(\mu\text{-Cl})(DAM)_2]^+$ and $[RhCl_2(CO)_2]^-$. It is not unreasonable to expect therefore that a similar process is occurring in the

(24) Otsuka, S.; Tatsuno, Y.; Miki, M.; Aoki, T.; Matsumoto, M.; Yoshioka, H.; Nakatsu, K. *J. Chem. Soc., Chem. Commun.* **1973**, 445.
(25) Mingos, D. M. P. *Transition Met. Chem.* **1978**, *3*, 1 and references therein.
(26) Post, B.; Schwartz, R. S.; Rankuchen, I. *Acta Crystallogr.* **1952**, *5*, 372.
(27) DeBoer, J. L.; Rogers, D.; Skapski, A. C.; Troughton, P. G. H. *Chem. Commun.* **1966**, 756. Muir, K. W.; Ibers, J. A. *Inorg. Chem.* **1969**, *8*, 1921. Mague, J. T. *Ibid.* **1969**, *8*, 1975.
(28) Bennett, M. J.; Donaldson, P. B. *Inorg. Chem.* **1977**, *16*, 655.
(29) Cowie, M.; Dwight, S. K. *Inorg. Chem.* **1979**, *18*, 1209.
(30) Olmstead, M. M.; Lindsay, C. H.; Benner, L. S.; Balch, A. L., submitted for publication. Balch, A. L., private communication.

transformation of **3** to **4**. In fact a model of $[Rh_2(CO)_2(\mu\text{-}CO)(\mu\text{-}Cl)(DPM)_2][RhCl_2(CO)_2]$, constructed from data made available to us by Professor Balch,[30] shows that the anion approaches the tricarbonyl cationic species (which we presume is structurally similar to complex **3a**), in such an orientation that chloride transfer from the anion to the cation is very feasible. We believe that the species resulting from Cl^- transfer by $[RhCl_2(CO)_2]^-$, i.e., $[RhCl(CO)_2]$ or the dimer $[RhCl(CO)_2]_2$, then abstracts a chloride ion from another cationic species **3a** to restart the process, resulting in a net chloride transfer reaction to yield a neutral dichloro dicarbonyl, sulfur dioxide bridged species, $[Rh_2Cl_2(CO)_2(\mu\text{-}SO_2)(DPM)_2]$, which then loses CO to yield complex **4**. Evidence supporting this dichloro dicarbonyl intermediate comes from our reactions of both *cis*- and *trans*-$[Rh_2Cl_2(CO)_2(DPM)_2]$ with SO_2 which also yield complex **4** when evaporated under an atmosphere of SO_2 (vide infra). Furthermore, we believe that it is much more likely that the relatively small species $[RhCl_2(CO)_2]^-$ is accomplishing the chloride transfer as opposed to any species containing the very bulky DPM ligand. Of course when chloride ion is added directly to a solution of **3a**, evaporation of this solution under SO_2 results in the quantitative conversion of **3a** to **4**. Furthermore, in the reaction of *trans*-$[Rh_2Cl_2(CO)_2(DPM)_2]$ with SO_2 the intermediate species is $[Rh_2(CO)_2(\mu\text{-}Cl)(\mu\text{-}SO_2)(DPM)_2][Cl]$. Concentration of this solution under SO_2 again yields complex **4** by recoordination of the chloride ion and CO loss (vide infra). Therefore the conversion of complex **3a** into **4** occurs in the presence of any chloride ion source. It is also of interest at this stage to note the differences between SO_2 and CO in these systems. In the presence of a chloride ion source the SO_2 adduct **3a** is unstable, yielding complex **4**, whereas the analogous tricarbonyl species $[Rh_2(CO)_2(\mu\text{-}Cl)(\mu\text{-}CO)(DPM)_2][X]$, $X = Cl^-$ or $[RhCl_2(CO)_2]^-$, are stable and readily isolated.

Efforts at characterizing the other so-called disproportionation products have met with little success. On the basis of $^{31}P\{^1H\}$ NMR spectra of the products in this reaction, we find, in addition to resonances due to **4**, at least three other unidentified resonances occur. The sum of their integrated intensities is approximately equal to that of complex **4**. It seems therefore that the second product in the reaction, species **5**, is unstable and is reacting further to yield the species observed in the NMR experiment. This is consistent with the fact that the relative intensities of the bands in the infrared spectra of the yellow product changed from sample to sample. However, it was noted that no carbonyl species were observed in the infrared spectra of the final yellow product.

(c) Reaction of $[Rh_2Cl_2(\mu\text{-}SO_2)(DPM)_2]$ with CO. Previously it had been reported[3] that the reaction of the neutral SO_2 "A-frame" complex **4** with CO yielded the tricarbonyl species *cis*-$[Rh_2Cl_2(CO)_2(\mu\text{-}CO)(DPM)_2]$. However, further investigations have shown that this tricarbonyl species is actually $[Rh_2(CO)_2(\mu\text{-}Cl)(\mu\text{-}CO)(DPM)_2][Cl]$ (**2b**) (see Scheme II). It is a 1:1 electrolyte in acetone and dichloromethane solutions, its $^{31}P\{^1H\}$ NMR spectrum[31] is identical with that of the BPh_4^- salt whose structure has been determined,[2,17] and its infrared spectrum is also similar to that of the BPh_4^- salt. Under vacuum, a solid sample of **2b** loses the bridging carbonyl ligand as indicated by its infrared spectrum which is then essentially identical with that of complex **1a** (see Table II). This species can therefore be formulated as $[Rh_2(CO)_2(\mu\text{-}Cl)(DPM)_2][Cl]$ (**1b**). A solution of **1b**, however, is a nonelectrolyte, and we believe that recoordination of the chloride ion occurs such that the species present in solution is actually the novel species *cis*-$[Rh_2Cl_2(CO)_2(DPM)_2]$ (**6**) (see Scheme II). Complex **6** can also be obtained directly by bubbling N_2 through a solution

Scheme II. Reaction of Binuclear Bis(diphenylphosphino)methane Complexes with CO and SO_2[a]

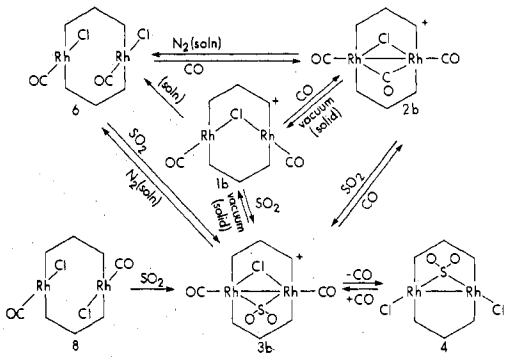

[a] For cationic species the anion is chloride.

of **2b**. The infrared spectra of complex **6** and of complex **1b** are very different and furthermore the $^{31}P\{^1H\}$ NMR spectrum of **6** is not similar to that of the BPh_4^- "A-frame" complex **1a**. This together with the conductivity differences between **1a** and **6** supports our assignment of this species as the *cis*-dicarbonyl complex. In addition, the infrared spectrum and elemental analysis of **6** are essentially identical with those of the trans analogue **8**. Our formulation of **6** as the cis species instead of the trans is based on chemical differences. Complex **6** is soluble in CH_2Cl_2 and acetone whereas the trans analogue **8** is extremely insoluble. Furthermore, **6** reacts readily and reversibly with CO in CH_2Cl_2 to give **2b**, whereas **8** does not react even after extended periods of time. One reviewer has suggested that the differences in solubility and reactivity of the "cis" and "trans" species may result not from cis–trans isomerism but from the degree of association of these species, with the more soluble "cis" species actually being the binuclear trans DPM complex analogous to the soluble *trans*-$[Rh_2Cl_2(CO)_2(DAM)_2]$[1,32] and the insoluble species being more highly polymerized. Although, on the basis of powder diffraction studies, the DPM and DAM species were found to be isomorphous,[32] the nature of the insoluble *trans*-$[Rh_2Cl_2(CO)_2(DPM)_2]$ was also a concern to us so we have carried out its X-ray structural determination[33] and have found that it is not polymeric but that it is rather similar to the DAM analogue. However, we concur that the unambiguous assignment of complex **6** as the cis species must await a structural determination.

Both the cis and trans species (**6** and **8**, respectively) react with SO_2 to yield the species $[Rh_2(CO)_2(\mu\text{-}Cl)(\mu\text{-}SO_2)(DPM)_2][Cl]$ (**3b**), which is assigned this structure on the basis of its conductivity (1:1 electrolyte) and its $^{31}P\{^1H\}$ NMR spectrum which shows only one phosphorus environment and which is identical with that of its BPh_4^- analogue **3a** (vide supra). In addition, when solutions of **6** and **8** are treated for prolonged periods of time with SO_2, complex **4** is obtained (see Scheme II).

(d) Reaction of *trans*-$[Rh_2Cl_2(CO)_2(DPM)_2]$ with SO_2. The reaction of the *trans*-dichlorodicarbonyl species (**8**) with SO_2 has been studied by monitoring, by infrared spectroscopy, the slow stepwise addition of SO_2. Initially species are observed which contain bridging carbonyl ligands (ν_{CO} 1740 cm^{-1}). Upon completion of the reaction none of these species is observed; instead only the symmetric SO_2-bridged species **3b** remains. In addition a solution containing the product of the SO_2 reaction with **8** is nonconducting for several minutes (although on the basis of spectral changes it is obvious that a reaction has taken place) after which time it becomes a 1:1

(31) Previously reported results (Cowie, M.; Dwight, S. K.; Sanger, A. R. *Inorg. Chim. Acta* **1978**, *31*, L407; **1979**, *32*, L56) are in error.

(32) Mague, J. T. *Inorg. Chem.* **1969**, *8*, 1975.
(33) Cowie, M.; Dwight, S. K., submitted for publication.

electrolyte. The above data are consistent with terminal attack of SO_2 and the formation of an intermediate species of the form

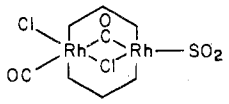

This species is then believed to lose Cl^- and to rearrange to the final product **3b**, having a bridging SO_2 ligand. We have obtained similar results when CS_2 instead of SO_2 is used.[34] In this case the chemistry parallels that which we propose for the SO_2 complex except that the intermediate species have longer lifetimes (days) so detailed spectroscopic measurements can be (and have been) made supporting our proposed scheme for the SO_2 reaction.

(e) Site of SO_2 Attack in $[Rh_2(CO)_2(\mu\text{-Cl})(DPM)_2]^+$. In these "A-frame" species there are two potential sites of attack, either directly at the enclosed site, bridging the metal centers, or at a terminal, exposed position remote from the bridging site. It has been shown that CO attacks **1a** terminally, forcing one of the previously coordinated carbonyl ligands into the bridge.[2,4] Likewise CO appears to attack the SO_2 "A-frame" complex **4** terminally since again no evidence was obtained for attack at the bridging site. In contrast, SO_2 appears to attack complex **1** directly at the bridging site, which has been shown to be open by the recent structural characterization of $[Rh_2(CO)_2(\mu\text{-Cl})(DPM)_2][BF_4]$.[5] In support of this mode of attack, the infrared spectra obtained during the slow stepwise addition of SO_2 to **1a** display no infrared bands assignable to bridging carbonyl species. On the basis of the analogous reaction of **1** with CO and the reaction of the *trans*-dichlorodicarbonyl species **8** with SO_2 (vide supra), both of which occur by terminal attack, we would have anticipated observing species with bridging CO bands in the infrared spectra, if attack of **1** with SO_2 were also terminal. Furthermore, even at −50 °C when the reaction is monitored by $^{31}P\{^1H\}$ NMR the only resonances observed are assignable to the symmetric species **1a** and **3a**. If attack were terminal, we would anticipate resonances assignable to an asymmetric species. We believe therefore that, on the basis of the above data, terminal attack of **1** by SO_2 can be ruled out, since no asymmetric species were detected. Furthermore we feel that it is unlikely that a facile rearrangement is operating since we can devise no simple rearrangement mechanism that would yield the symmetric bridged species **3a** from terminal attack. The reason for the different modes of attack of CO and SO_2 in complex **1** is at the present time not obvious.

Although we now understand much about the modes of attack and coordination of SO_2 in these binuclear systems as well as some of the subsequent chemistry of these SO_2 complexes, there are still some unanswered questions remaining, particularly relating to the differences in the chemistries of SO_2 and CO in these systems. It is anticipated that our continuing investigations in this area will help answer some of these unanswered questions and will extend our understanding of the chemistry of binuclear metal complexes.

Acknowledgment. The authors thank the National Science and Engineering Research Council of Canada and the University of Alberta for financial support, NSERC for a scholarship to S.K.D., Dr. A. R. Sanger for supplying the crystals of complex **4**, and Professor A. L. Balch for communication of his results prior to publication.

Registry No. **1a**, 67202-35-1; **1b**, 71647-00-2; **2b**, 71647-01-3; **3a**, 68080-76-2; **3b**, 71646-99-6; **4**, 69063-81-6; **6**, 22427-58-3; **8**, 22427-58-3; $[RhCl(COD)]_2$, 12092-47-6.

Supplementary Material Available: Table IX, showing the idealized hydrogen parameters and a listing of the observed and calculated structure amplitudes (25 pages). Ordering information is given on any current masthead page.

(34) Cowie, M.; Dwight, S. K., to be submitted for publication.

Contribution from the Theoretical Division, Los Alamos Scientific Laboratory, Los Alamos, New Mexico 87545, and the Department of Chemistry, Harvard University, Cambridge, Massachusetts 02138

Stereochemical Rigidity and Isomerization in B_4H_4 and B_4F_4. A Theoretical Study

DANIEL A. KLEIER,*[1] JOSEF BICERANO, and WILLIAM N. LIPSCOMB

Received August 27, 1979

The degenerate rearrangement of both tetrahedral B_4H_4 and B_4F_4 along a least-motion pathway passes through a square-planar midpoint structure. This rearrangement is accompanied by an orbital crossing of the HOMO–LUMO type which is responsible for the imposition of a sizable barrier to the process. Both approximate and ab initio calculations including correlation were performed to characterize the pathway for these rearrangements. For B_4H_4 a barrier of approximately 85 kcal/mol is calculated while a smaller barrier is predicted for B_4F_4. For both molecules the square midpoint structure may be a stable intermediate along the reaction pathway.

As part of a continuing study of rearrangements in closo boron hydrides,[2-4] we report here on the nature of the stereochemical rigidity in B_4X_4 (X = H, F). The degenerate rearrangement of B_4X_4 provides the ultimate example of a diamond–square–diamond (dsd) transformation[5] in a small system (Scheme I). Previous theoretical studies have not considered the nature of the square midpoint structure nor the nature of the electronic reorganization required for the dsd transformation in B_4X_4.

Scheme I

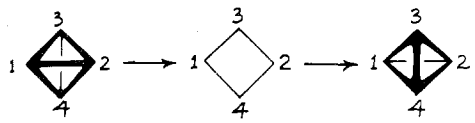

(1) Camille and Henry Dreyfus Teacher-Scholar Grantee, 1979–1984. Address correspondence to Thompson Chemical Laboratory, Williams College, Williamstown, MA 01267.
(2) D. A. Kleier, D. A. Dixon, and W. N. Lipscomb, *Inorg. Chem.*, **17**, 166 (1978).
(3) D. A. Kleier and W. N. Lipscomb, *Inorg. Chem.*, **18**, 1312 (1979).
(4) I. M. Pepperburg, T. A. Halgren, and W. N. Lipscomb, *J. Am. Chem. Soc.*, **97**, 1284 (1975).
(5) W. N. Lipscomb, *Science*, **153**, 373 (1966).

0020-1669/80/1319-0216$01.00/0